Voltage-dependent Slowing of K Channel Closing Kinetics by Rb^+

SALVADOR SALA and DONALD R. MATTESON

From the Department of Biophysics, University of Maryland School of Medicine, Baltimore, Maryland 21201; and the Marine Biological Laboratory, Woods Hole, Massachusetts 02543

ABSTRACT We have studied the effect of Rb^+ on K channel closing kinetics in toadfish pancreatic islet cells. These channels are voltage dependent, activating at voltages positive to −10 mV. The channels also inactivate upon prolonged depolarizations, and the inactivation time course is best fit by the sum of two exponentials. Instantaneous current–voltage relationships show that external Rb^+ enters the channel as easily as K^+, but carries less current. In the voltage range from −140 to −50 mV, the closing time course of the channels can be fit with a single exponential. When Rb^+ is present in the external solution the channels close more slowly. The magnitude of this Rb^+ effect is voltage dependent, decreasing at more negative voltages. Similarly, when the internal solution contains Rb^+ instead of K^+ the closing time constants are increased. The effect of internal Rb^+ is also voltage dependent; at voltages positive to −80 mV the closing time constant in internal Rb^+ is slower than in K^+, whereas at more negative voltages the difference is negligible. With internal Rb^+, the relationship between the closing time constant and voltage is best fit with two exponential components, suggesting the presence of two distinct voltage-dependent processes. The results are discussed in terms of a model of the K channel with two internal binding sites, and we conclude that Rb^+ produces its effects on channel gating by binding to a site in the pore.

INTRODUCTION

In spite of early reports of the lack of effects of permeant ions on channel gating (Hodgkin and Huxley, 1952; Chandler and Meves, 1965), it has recently become evident that there are significant interactions between the ion permeation pathway and gating in several types of ionic channels. The effect was first observed in acetylcholine receptor channels by Van Helden, Hamill, and Gage (1977), who found that the channel open time varied with the species of ion carrying the current. Marchais and Marty (1979) later extended these results and proposed that changes in channel open time were mediated by binding of permeant ions in the pore. Similar effects of permeant ions on channel gating have been reported in inward rectifier K channels (Hagiwara and Yoshii, 1979), squid delayed rectifier K channels (Swenson and Armstrong, 1981; Matteson and Swenson, 1986), Ca channels (Nelson, French,

Address reprint requests to Dr. Donald R. Matteson, Department of Biophysics, University of Maryland at Baltimore, 660 West Redwood Street, Baltimore, MD 21201.

J. GEN. PHYSIOL. © The Rockefeller University Press · 0022-1295/91/09/0535/20 $2.00
Volume 98 September 1991 535–554

and Krueger, 1984), K channels in lymphocytes (Cahalan, Chandy, DeCoursey, and Gupta, 1985), delayed rectifiers in frog skeletal muscle (Spruce, Standen, and Stanfield, 1989), and Ca-activated K channels in rat skeletal muscle (Demo and Yellen, 1990) and taenia coli myocytes (Hu, Yamamoto, and Kao, 1989).

In a previous study of gating in the squid delayed rectifier K channel, Matteson and Swenson (1986) proposed that permeant ions such as Rb^+ or K^+ slow channel gating by occupying a site within the pore, and this idea was called the occupancy hypothesis. Two main observations led to this conclusion: (*a*) only *permeant* monovalent cations affected gating, and (*b*) there was a correlation between monovalent occupancy of the channel and closing kinetics. However, this hypothesis was recently challenged. Clay (1988) reported that the voltage dependence of the slowing effect of Rb^+ or Cs^+ on K channel closing in the squid axon was inconsistent with the occupancy hypothesis, and proposed that the ions directly affected the gating apparatus by acting at a site on the *external* surface of the channel. In contrast, recent studies of the Ca-activated K channel have shown that Cs^+ ions increase the channel open time *more* at membrane potentials that increase the Cs^+ block of the channel (Demo and Yellen, 1990), a result that is consistent with the occupancy hypothesis.

We have further studied the effect of Rb^+ on K channel gating using voltage-dependent K channels in toadfish pancreatic islet cells. These cells have a consistently large population of voltage-dependent K channels, with permeation characteristics resembling K channels found in other preparations, such as the K channel in squid giant axons (Oxford and Adams, 1981; Wagoner and Oxford, 1987) and the Ca-activated K channel (Blatz and Magleby, 1984). To gain additional information about the location of the site where Rb^+ produces its slowing effect, we studied the voltage dependence of channel closing kinetics. We found that either external or internal Rb^+ ions slow K channel closing in a voltage-dependent manner. With internal Rb^+, the voltage dependence of channel closing is best fit with the sum of two exponentials, suggesting that voltage affects channel gating in two distinct ways.

A preliminary report of these results has been presented elsewhere (Matteson and Sala, 1990).

METHODS

Preparation and Culturing of Toadfish Islet Cells

The primary, secondary, and usually one or two tertiary islets were dissected out of the mesentery of toadfish (*Opsanus tau*). The islets were trimmed of connective tissue and washed in a divalent-free Spinner salt solution. To obtain single islet cells, the islets were minced in a solution of Spinner salts containing 3 mg/ml dispase, and the tissue was triturated for ~20 min to disperse the endocrine cells. The resulting cell suspension was then washed three times in RPMI 1640 tissue culture media, and the cells were plated onto slivers of coverslips sized to fit our experimental chamber. The cells were incubated at room temperature (20–21°C) in a complete culture medium made of HEPES-buffered RPMI supplemented with 10% fetal bovine serum, 300 mg/ml glutamine, 100 U/ml penicillin, and 100 μg/ml streptomycin. Cells were used for up to 1 wk.

Patch-Clamp Recording

Our use of the whole-cell variation of the patch-clamp technique was as previously described (Hiriart and Matteson, 1988). In recent experiments, pulse generation and data acquisition were controlled by a Compaq 386 computer through an interface of our own design. The interface utilizes a 16-bit A/D converter that can operate at rates up to 100 kHz. A programmable pulse generator produces pulse intervals of variable amplitude (using a 14-bit D/A converter) and variable duration (from 15 μs to 83 s). Low resistance patch electrodes (1–2 MΩ) were pulled from Corning N51A or soda-lime glass. Series resistance compensation was used. The output of the patch clamp was filtered with an 8-pole Bessel filter at 10 kHz, and usually sampled at 50 kHz. The holding potential was −80 mV in all experiments. The linear components of current were subtracted by the computer with a P/2 procedure using positive control pulses from −120 mV (cf. Armstrong and Bezanilla, 1974). All experiments were performed at room temperature (20–21°C).

TABLE I

Recording Solutions

External solution*	NaCl	KCl	RbCl	NH_4Cl	$CaCl_2$	HEPES‡	TTX
A	47	100	—	—	2	10	200
B	47	—	100	—	2	10	200
C	47	—	—	100	2	10	200
D	147	—	—	—	2	10	200
E	142	5	—	—	2	10	200
F	117	30	—	—	2	10	200

Internal solution	KCl	KF	KGl§	RbCl	RbF	RbGl§	$MgCl_2$	EGTA	HEPES‖
G	30	—	105	—	—	—	2	10	10
H	30	25	80	—	—	—	—	10	10
I	—	—	—	30	25	80	—	10	10

*Concentrations are in millimolar, except for TTX which is in nanomolar.

‡External pH adjusted to 7.4 with NaOH.

§Glutamate.

‖HEPES and EGTA were neutralized to pH 7.15 with KOH (solutions G and H), or with RbOH (solution I).

Solutions

The compositions of the ionic solutions used in these experiments are shown in Table I. Liquid junction potentials between the internal and external solutions were found to be <5 mV and therefore voltages were not corrected for these potentials. Na currents were eliminated by using tetrodotoxin (TTX, 200 nM), and Ca currents were minimized by using only 2 mM Ca externally. Ca channel blockers were not used because many of them are known to directly affect K channels (e.g., DeCoursey, Chandy, Gupta, and Cahalan, 1987). Culture media and other reagents were obtained from the following sources: Spinner salts, RPMI 1640, penicillin/streptomycin, and TTX from Sigma Chemical Co. (St. Louis, MO), fetal bovine serum from Flow Laboratories, Inc. (McLean, VA), dispase from Boehringer Mannheim Corp. (Indianapolis, IN), and glutamine from Gibco Laboratories (Grand Island, NY).

Data Analysis

Two procedures have been used to characterize the K channel closing kinetics: tail current measurements and a double pulse procedure (cf. Matteson and Swenson, 1986). Over the voltage range from −140 to −50 mV, both procedures usually yield data that can be well fit by a single exponential. Single exponentials were fit to the data using a weighted least-squares fitting routine, and the time constant was used as a measure of the channel closing kinetics. The time courses of inactivation and recovery from inactivation were fit to the sum of two exponentials plus a nonzero baseline using a Levenberg-Marquardt iterative procedure.

Barrier Modeling

K channels were modeled as having an energy profile with three barriers and two wells. The open channel *I-V* relationships predicted by this model were calculated using the method described in Begenisich and Cahalan (1980). The frequency factor used in the calculations of the rate constants was 10^{11} $mol^{-1}s^{-1}$ for transitions from bulk solution to the pore, and 10^{13} s^{-1} for all other transitions (cf. Lewis and Stevens, 1979). To account for the electrostatic repulsion exerted at one site by an ion sitting at an adjacent site, rate constants were multiplied (or divided) by a repulsion factor of 1–10 (Hille and Schwarz, 1978).

The model has the following adjustable parameters: five energy levels for each different permeant cation (K^+ and Rb^+ in our experiments), five independent electrical distances, and a factor proportional to the number of channels. Currents were calculated from the model using a program written in C, and were compared with the instantaneous current–voltage (IIV) relationship. To estimate the parameters of the model we used an iterative procedure to minimize the squared deviations between the model predictions and the IIV data. With this procedure we found that by using different initial conditions, the procedure can locate several local minima, so that many sets of parameters accurately fit the data. Given a set of parameters, the model was then used to calculate the probability that either of the binding sites is occupied by a monovalent cation.

RESULTS

Inactivating K Currents

We have found that toadfish pancreatic islet cells contain a population of inactivating, voltage-dependent K channels. Macroscopic currents generated by 100-ms steps to the various potentials are shown in Fig. 1 *A*. The activation kinetics of the current are clearly voltage dependent: at +30 mV the current rises to a peak in ~12 ms, whereas at +90 mV the current reaches a peak in ~6 ms. Fig. 1 *B* is a peak *I-V* relationship for the outward current. The channels begin to activate at about −10 mV, and at voltages positive to about +30 mV the conductance reaches a maximum of 22.4 ± 1.4 nS (n = 3). We will show later that selectivity measurements indicate that these currents flow through K channels (cf. Fig. 3).

Following activation the K current declines (or inactivates) along a double exponential time course during the maintained depolarization. Fig. 2 *A* shows the current generated by a 740-ms step to +70 mV. We have fit the inactivation time course with the sum of two exponentials (continuous line) or with a single exponential (dashed line) using a nonzero baseline. The double exponential fit is clearly better. In four cells, τ_{fast} averaged 32.6 ± 9.2 ms and τ_{slow} was 236 ± 31 ms.

As we will describe below, we used a double pulse procedure to characterize the rate of K channel closing. With this procedure, several (six to nine) iterations of a double pulse protocol must be given to estimate the closing rate. To assure that time courses related to K channel inactivation would not affect our measurement of closing kinetics, we had to be sure that the time interval between iterations of the double pulse procedure (i.e., the cycle period) was long enough to allow for recovery from inactivation. The rate of recovery from inactivation was studied as shown in Fig. 2 *B*. The inset illustrates the pulse procedure, which consisted of an inactivating

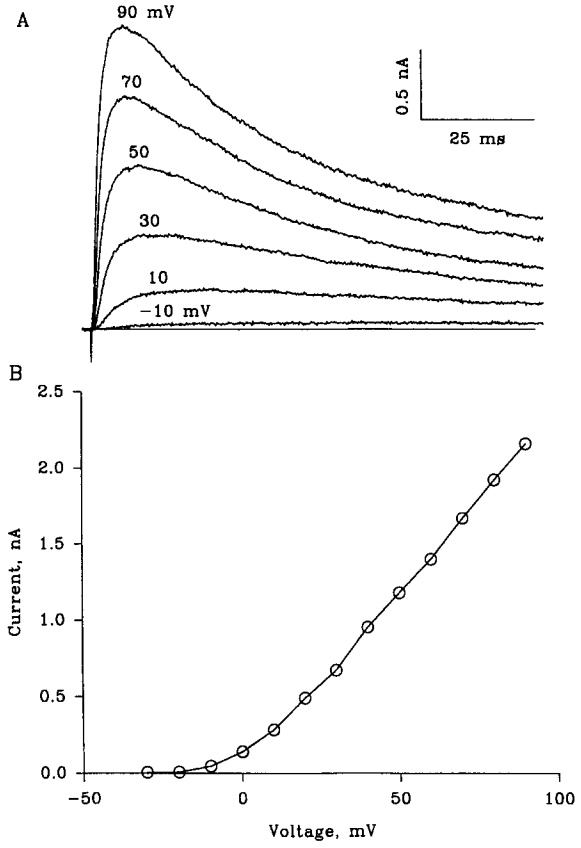

FIGURE 1. Currents generated by inactivating, voltage-dependent K channels in toadfish pancreatic islet cells. (*A*) 100-ms steps were given from a holding potential of −80 mV to the indicated potentials. After peak activation, the current declines along a double exponential time course (τ_{fast} = 32.6 ± 9.2 ms and τ_{slow} = 236 ± 31 ms [n = 4] at +70 mV). (*B*) Peak *I-V* relationship taken from the records shown in *A*. The data show that the channels begin to activate at about −10 mV. External solution E. Internal solution H.

prepulse (P1) to +70 mV for 500 ms. After a variable recovery interval at the holding potential, a second pulse (P2) was given to measure the noninactivated current. Fig. 2 *B* illustrates recovery data for four different cells. The recovery time course is best fit by the sum of two exponentials, and Table II shows estimates of the time constants of the fast and slow recovery components. Although there is some variability in the rate of recovery from inactivation, the channels appear to be fully recovered after 10 s at −80 mV. Therefore, the cycle period was set at 10–30 s for all experiments in this study.

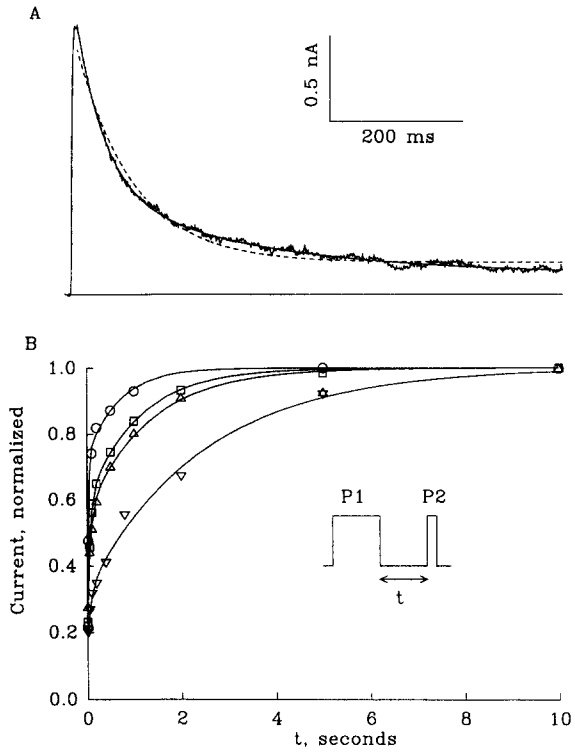

FIGURE 2. Time course of inactivation and recovery from inactivation. (*A*) Current obtained with a 740-ms pulse to +70 mV. The current has been fit to a single exponential (*dashed line*) or to the sum of two exponentials (*continuous line*). (*B*) The pulse procedure used to study recovery from inactivation (shown in the inset) consisted of an inactivating prepulse (*P1*) to +70 mV for 500 ms. After a variable recovery interval at −80 mV, a second pulse (*P2*) was given to measure the noninactivated current. The magnitude of the noninactivated current is plotted as a function of the recovery interval. The four different symbols plot recovery data from four separate cells, and the lines are fits of the sum of two exponentials. External solution F. Internal solution H.

Permeation and Selectivity

Some properties of ion permeation and selectivity in channels can be assessed by examining the open channel *I-V* relationship (Hille and Schwarz, 1978). With macroscopic current recordings, the shape of the open channel *I-V* is assessed by measuring the IIV relationship. The inset in Fig. 3 *C* illustrates the pulse protocol used to obtain IIVs. P1, a 5-ms pulse to +70 mV, activates the K channels. The voltage was then stepped to a new level (P2) and the "instantaneous" current was measured 100–200 μs after the step, at a time corresponding to the largest absolute value of the current. Currents generated with this protocol in 100 K (solution A) are shown in Fig. 3 *A*, and were used to construct the curve labeled 100 K in Fig. 3 *C*. Under these conditions the potassium equilibrium potential is about −7.5 mV, which

TABLE II

Time Constants of Recovery from Inactivation

Cell	τ_{fast}	τ_{slow}
SE029A, cell 2	0.029*	0.676
SE029B, cell 6	0.190	3.13
SE029C, cell 9	0.070	1.32
SE029C, cell 10	0.057	1.11

*Time constants are in seconds.

is close to observed reversal potential of ~0 mV, showing that the current flows through K channels.

To compare permeation by several different cations, we measured IIVs in a single cell in the presence of four different external solutions (Fig. 3 *C*). The curve labeled 100 Na was obtained in external solution D, with Na^+ as the main external cation. The other curves were obtained after substituting 100 mM of the test cation for 100

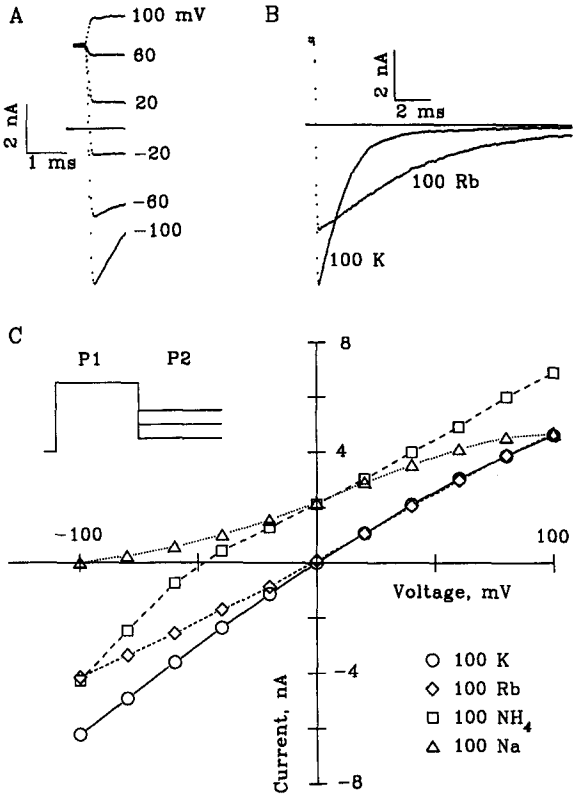

FIGURE 3. Instantaneous *I-V* curves obtained in a single cell in the presence of four external solutions. (*A*) Currents obtained with the pulse protocol shown in the inset of *C*. In this protocol, P1 (a 5-ms pulse to +70 mV) activates the K channels. The current is then measured just after stepping the potential to P2, which is varied from −100 to +100 mV. For each trace, the current was sampled 0.2 ms before P1 to provide a base line and the sampling was then turned off. Sampling was turned back on 0.2 ms before the end of P1. The level of P2 is indicated to the right of each trace. External solution A. (*B*) Currents recorded using a P2 of −100 mV in two external solutions: solution A containing 100 mM K, or solution B with 100 mM Rb. Note that the tail current decays much more slowly in the presence of external Rb^+. (*C*) Instantaneous *I-V* curves obtained by plotting the magnitude of the instantaneous current vs. the P2 voltage. The curve labeled 100 Na was obtained in external solution D. The other curves were obtained after substituting 100 mM of a test cation for 100 mM Na in solution D (solutions A–C). In this experiment, the order of solution changes was 100 K, 100 NH_4, 100 Na, 100 Rb, and then, to check for reversibility, a return to 100 K. The data from the two runs in 100 K were similar and were therefore averaged for this figure. Internal solution G.

mM Na^+ in solution D (these are solutions A–C in Table I). The reversal potential reflects the ability of an ion to enter the channel, and the shape of the *I-V* curve reflects the ability of the ion to carry current (Hille and Schwarz, 1978). From Fig. 3, it is clear that Na^+ ions do not go through the channels, because there is no inward current with Na^+ as the only external monovalent cation (curve labeled 100 Na). NH_4^+ ions do not enter the channel readily (as indicated by the negative reversal

potential), but the inward current carried by NH_4^+ is large. Of most interest to us was the action of external Rb^+. Fig. 3 *B* is a comparison of inward tail currents in either 100 K or 100 Rb. The initial magnitude of the current is smaller in 100 Rb, and the subsequent tail current is slower. The reversal potential in 100 Rb was nearly the same as the reversal potential in 100 K (Fig. 3 *C*), demonstrating that Rb^+ enters the channel as readily as K^+. However, the inward current in 100 Rb, carried by Rb^+ ions, is less than the inward current in 100 K, which is carried by K^+, suggesting that Rb^+ binds more tightly in the channel. These permeation characteristics are similar to the properties of voltage-dependent K channels in squid and other preparations (Oxford and Adams, 1981; Matteson and Swenson, 1986; Spruce et al., 1989).

Closing Kinetics: Double Pulse Protocol vs. Tails

The traditional method of measuring channel closing kinetics using macroscopic currents is through the use of tail currents (Hodgkin and Huxley, 1952). In many of our experiments we had to estimate closing kinetics under conditions where there would be little or no tail current (e.g., at a negative voltage with no external permeant cations). Therefore, we used a double pulse procedure to estimate closing kinetics (cf. Matteson and Swenson, 1986), and in Fig. 4 we compare double pulse and tail current measurements. Fig. 4 *A* shows data obtained with the two methods in the same cell. In both methods the K channels are first opened with a 10-ms step to +70 mV. After repolarization we measure a tail current which decays as channels close. These tails are well fit by a single exponential, and the time constant provides a measure of channel closing rate. In the double pulse procedure, the membrane is repolarized for a variable period of time to allow channels to close, and a second pulse is then given. The instantaneous increase in current following the second step is a measure of the number of channels still open. The dashed line in Fig. 4 *A*, drawn through the second pulse currents, reflects the rate of channel closing. It is apparent from this figure that the dotted line and the tail current have similar kinetics. Fig. 4 *B* and Table III compare time constants obtained with the two methods in several cells at a range of membrane potentials. The two methods provide similar estimates of closing kinetics. In all of the following figures, we have used the double pulse procedure to study K channel closing kinetics.

External Rb^+ and K Channel Closing

As in the squid delayed rectifier K channel, external Rb^+ dramatically slows K channel closing in toadfish islet cell K channels. Fig. 5 shows the closing kinetics with and without external Rb^+ in the same cell. The straight lines drawn through the data points are single exponential fits to the first six to eight data points. When the channels were allowed to close at −60 mV (Fig. 5 *A*), the closing time constant was 33.5 ms in 100 mM Rb^+ and 3.25 ms in 5 mM K. Thus, Rb^+ slowed closing ~10 times at −60 mV, and the effect was completely reversible (not illustrated).

To further characterize the Rb effect we have examined its voltage dependence. Fig. 5 *B* shows that at −120 mV the closing time constant was 0.56 ms in our control external solution and 1.43 ms in 100 Rb^+. Thus, channel closing was slowed only 2.55

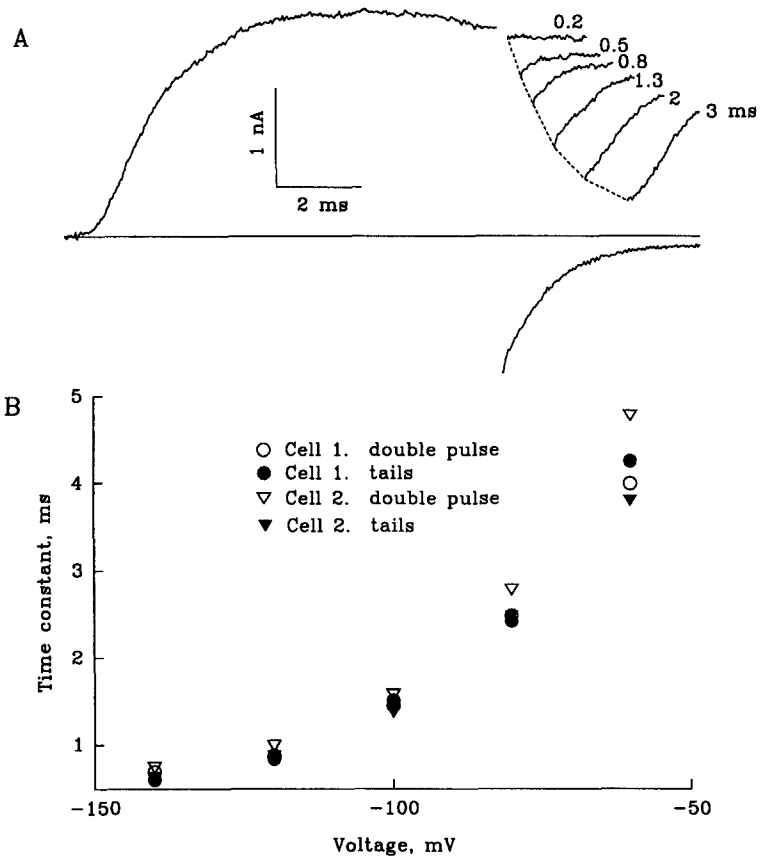

FIGURE 4. Comparison of closing kinetics obtained with tails and a double pulse procedure. (*A*) Kinetic data obtained with the two methods in a single cell. In both methods, the K channels are first opened with a 10-ms step to +70 mV. After repolarization to −80 mV, we measure a tail current which decays as channels close. These tails are well fit by a single exponential, and the time constant provides a measure of channel closing rate. In the double pulse procedure the membrane is repolarized for a variable period of time to allow channels to close, and a second pulse is then given (pulse protocol similar to that shown in Fig. 2). The instantaneous increase in current after the second step is a measure of the number of channels still open. Six second pulse currents are shown in *A*, and the interval between pulses is indicated next to each trace. The dashed line, drawn through the second pulse currents, reflects the rate of channel closing. (*B*) Time constants vs. voltage. The abscissa is either the voltage where the tails were measured or, in the double pulse procedure, the voltage between pulses. The time constants obtained with the two methods in two different cells are similar. External solution F. Internal solution H.

times at −120 mV, compared with the 10-fold slowing at −60 mV. Data covering a more complete voltage range are shown in Fig. 6. Fig. 6*A* is a plot of the reciprocal of the closing time constant, which is a measure of the channel closing rate, as a function of voltage. Hyperpolarization increases the closing rate in both solutions

TABLE III

Closing Time Constants

Cell	Method	−60 mV	−80 mV	−100 mV	−120 mV	−140 mV
SE029A,1	Tails	4.55	2.79	1.67	0.99	0.71
	DP	5.13	2.87	1.72	1.05	0.81
SE029A,2	Tails	3.94	2.25	1.43	0.90	0.60
	DP	4.77	3.02	1.76	0.99	0.81
SE029B,1	Tails	4.25	2.45	1.50	0.84	0.60
	DP	3.99	2.48	1.44	0.88	0.69
SE029C,1	Tails	3.82	2.47	1.37	0.87	0.63
	DP	4.79	2.78	1.57	0.99	0.74

This table gives the values of the closing time constant, in milliseconds, at various voltages estimated by two different methods: tails and a double pulse (DP) procedure.

(Fig. 6 *A*), but the effect of voltage is larger in Rb^+. The voltage dependence of the Rb effect can be seen clearly in Fig. 6 *B*, which plots the ratio of the closing time constant in Rb^+ to that in the control solution. A similar voltage dependence was observed in eight other cells (Table IV).

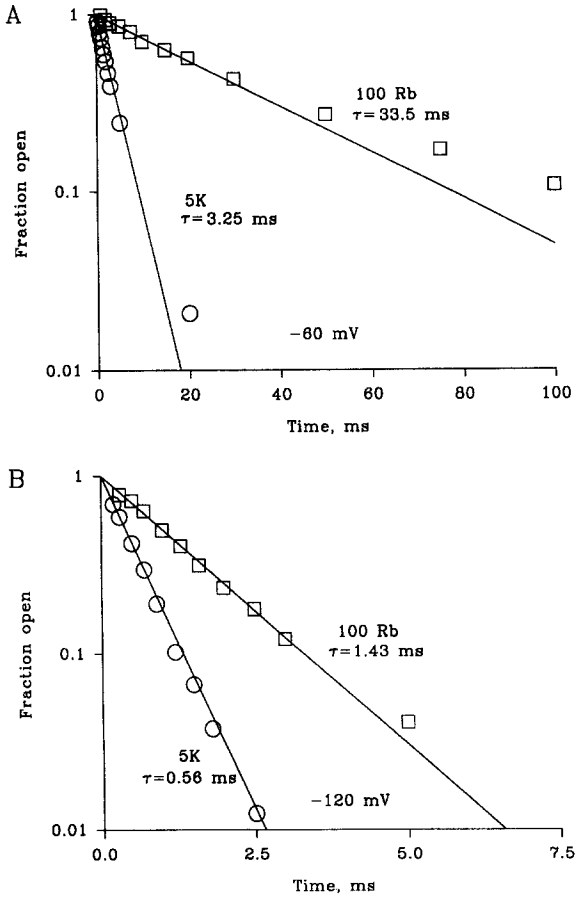

FIGURE 5. Closing kinetics characterized with the double pulse protocol. The symbols plot normalized data from the double pulse protocol and the straight lines are single exponential fits to the first six to eight data points. The data have been normalized to the initial amplitude of the fitted exponential, and therefore provide an estimate of the fraction of open channels. Closing kinetics were characterized in two different external solutions: 5 mM K (control) or 100 mM Rb (solutions E and B, respectively). (*A*) K channel closing kinetics at −60 mV, where 100 mM Rb slowed closing by a factor of 10.3. (*B*) K channel closing at −120 mV, where 100 mM Rb slowed closing by a factor of 2.55. Internal solution H.

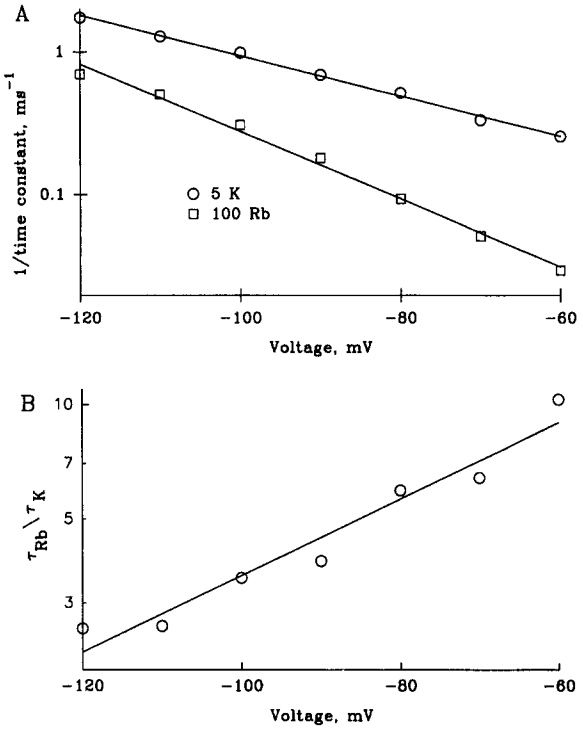

FIGURE 6. (*A*) Voltage dependence of closing kinetics with and without external Rb^+. The reciprocal of the closing time constant (obtained as shown in Fig. 5) is plotted vs. voltage for two different external solutions: external solution E (5 K) or B (100 Rb). Internal solution H. (*B*) Voltage dependence of the external Rb^+ effect. The ratio of the time constant in 100 Rb to the time constant in 5 K is plotted as a function of membrane potential. The straight line is an exponential fit of the data, and the slope corresponds to an *e*-fold change in the ratio of the time constants for a 43-mV change in membrane potential.

Internal Rb^+ and K Channel Closing

If external Rb^+ ions slow channel closing by directly interacting with the gate at an external site we would not expect internal Rb^+ to affect channel gating. To test for an effect of internal Rb^+ ions, the closing kinetics in internal K^+ were compared with the kinetics in internal Rb^+ (Fig. 7). At relatively positive voltages (from −80 to −50 mV) the time constants with internal Rb^+ are significantly slower than with internal K^+. At more negative voltages (−140 to −100 mV) the difference is negligible. With internal Rb^+, the relationship between closing rate and voltage must be fit with two

TABLE IV

Voltage Dependence of the Slowing Effect of External Rb

Cell	τ_{Rb}/τ_K at −60 mV	τ_{Rb}/τ_K at −120 mV
AU318A, cell 1	7.29	3.01
AU318A, cell 2	4.81	2.35
FE069B, cell 4	10.3	2.55
JL1790, cell 1	5.25	2.28
JL1790, cell 2	6.51	2.34
JL1890, cell 1	5.79	2.73
JL1990, cell 1	7.75	4.00
JL2190, cell 1	9.55	4.11
JL2390, cell 1	6.04	2.78

This table shows the ratio of the closing time constant in external Rb^+ (τ_{Rb}) to the time constant in the control solution (τ_K) at two voltages: −60 and −120 mV.

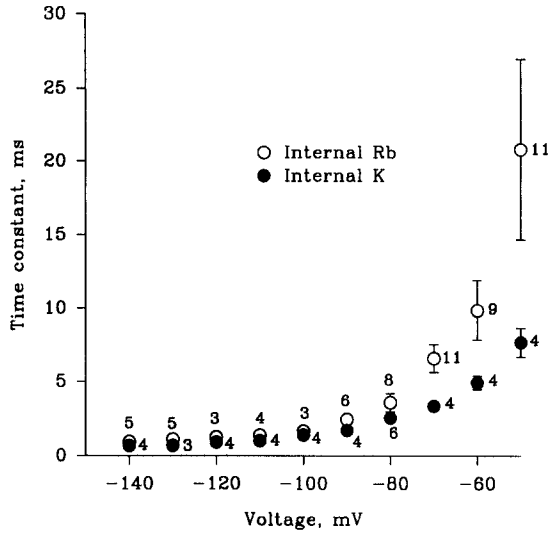

FIGURE 7. Closing time constant as a function of voltage with either K^+ or Rb^+ as the internal permeant cation (solution H or I, respectively). The data are plotted as the mean time constant (±SD) averaged for the indicated number of cells. The closing kinetics in the presence of internal Rb^+ are markedly slower at the more positive voltages (−70 to −50 mV). At more negative voltages the difference becomes negligible. External solution E.

exponential components (Fig. 8). This voltage dependence is consistent with the idea that Rb^+ slows closing by acting at a site in the channel. At more positive voltages the Rb^+ occupancy of the channel would be relatively high and the slowing effect of Rb^+ would be large. Hyperpolarization would decrease occupancy by "pulling" the ion into the cell interior, thereby reducing the effect of Rb^+ on gating. The dual effect of voltage on K channel closing, suggested by the results of Fig. 8, can be interpreted in the following way. At positive voltages (−90 to −50 mV) changes in voltage alter closing kinetics primarily by changing the Rb^+ occupancy of the channel. At more

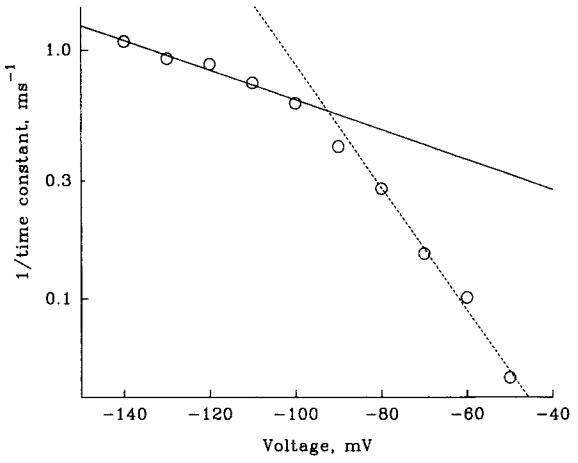

FIGURE 8. The symbols plot the reciprocal of the closing time constant vs. the membrane potential for the internal Rb^+ data of Fig. 7. The straight lines are single exponential fits through the five most negative points (*solid line*) or the five most positive points (*dashed line*). The data are clearly well fit by two exponential components. We interpret these data as indicating that at relatively positive voltages, changes in the membrane potential alter closing kinetics primarily by changing the Rb occupancy of the channel. At more negative voltages, changes in voltage alter closing kinetics as a result of the intrinsic voltage dependence of channel gating. External solution E. Internal solution I.

negative voltages where the Rb^+ occupancy is low, the direct effect of voltage on the channel's voltage sensor becomes apparent.

Instantaneous I-V Curve with Internal Rb^+

Estimates of the probability that a binding site in the channel is occupied by an ion can be obtained from a barrier model of ion permeation (Hille and Schwarz, 1978; Begenisich and Cahalan, 1980). To apply a barrier model to our results, we needed to measure the open channel *I-V* relationship in the presence of internal Rb^+. Fig. 9 shows the instantaneous *I-V* curve obtained with 100 mM internal Rb^+ and 5 mM external K^+. The same pulse protocol as shown in Fig. 3 was used. Under these conditions the outward current is carried by Rb^+, the small inward current is carried by K^+, and the current reverses at about −75 mV. Fits of a three-barrier, two-site model to this data, and to the instantaneous *I-V* curve obtained in either external Rb^+ or external K^+ (Fig. 3), were used to estimate the probability of site occupancy as described in the Discussion.

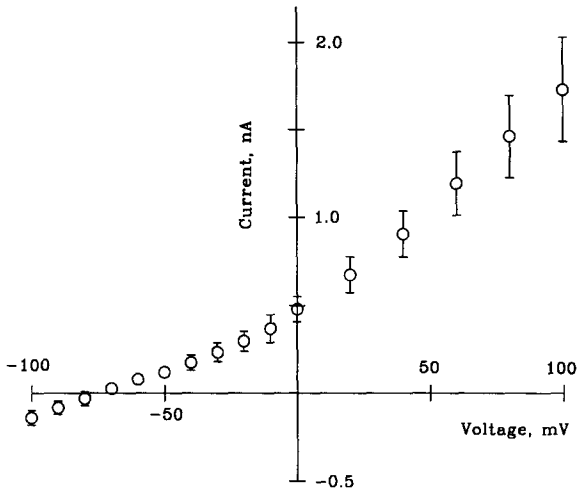

FIGURE 9. Instantaneous *I-V* curve in the presence of internal Rb^+. These data were obtained with a pulse protocol similar to the one shown in the inset of Fig. 3 *C*. The data points are the mean (±SD) currents from five cells. External solution E. Internal solution I.

DISCUSSION

The results of this study show that Rb^+ ions readily enter K channels in toadfish pancreatic islets cells, bind relatively tightly in the pore, and dramatically slow channel closing kinetics. The slowing effect is produced by internal as well as external Rb^+, and in both cases the effect of Rb^+ is reduced by hyperpolarization. As discussed in the following paragraphs, these results are consistent with the occupancy hypothesis, which states that Rb^+ affects channel gating by binding at a site in the pore and inhibiting channel closing.

Entry and Binding of Rb^+ Ions in the Channel

Our measurements of the open channel *I-V* relationship in toadfish K channels (Fig. 3) show that substitution of external Rb^+ for K^+ produces little change in the reversal

potential, indicating that these two ions enter the channel equally well. However, Rb^+ carries less current than K^+, so it must bind more tightly in the channel. Similar results have been obtained in the delayed rectifier in squid giant axons (Swenson and Armstrong, 1981; Matteson and Swenson, 1986; Wagoner and Oxford, 1987) and in frog skeletal muscle (Spruce et al., 1989), in the Ca-activated K channel in rat skeletal muscle (Blatz and Magleby, 1984; Demo and Yellen, 1990) and taenia coli myocytes (Hu et al., 1989), and in the ATP-blockable K channels in pancreatic β cells (Ashcroft, Kakei, and Kelly, 1989). In agreement with our reversal potential measurements, permeability ratios (P_{Rb}/P_K) close to 1.0 have been found in the delayed rectifier of rat skeletal muscle (Gay and Stanfield, 1978; Spruce et al., 1989), at the frog node of Ranvier (Hille, 1973), and in GH3 anterior pituitary cells (Oxford and Wagoner, 1989). In addition, many of these studies have indicated that the currents carried by Rb^+ are much smaller than those carried by K^+. Qualitatively similar results have been reported in cases where P_{Rb}/P_K is less than one. For example, in the Ca-activated K channel, Hu et al. (1989) reported a value of 0.65 for P_{Rb}/P_K, but a conductance ratio (g_{Rb}/g_K) of only 0.31, and concluded that Rb^+ ions bind in the pore. Ashcroft et al. (1989) found that P_{Rb}/P_K was ~0.7 for ATP-blockable K channels in rat pancreatic β cells. They also found that small amounts of external Rb^+ could block inward K currents, but the block was decreased at negative voltages. As a result they concluded that Rb^+ is a "permeant blocker" of the channel. All of the results discussed here demonstrate that Rb^+ ions readily enter K channels and bind relatively tightly in the pore.

Rb^+ Ions Slow K Channel Closing Kinetics

In addition to the ability of Rb^+ to bind tightly in the pore, we have found that Rb^+ ions slow the closing kinetics of toadfish K channels. Many of the studies cited in the previous paragraph also reported that K channels close more slowly in the presence of Rb^+ ions. For example, K channel tail currents decay more slowly in the presence of Rb^+ in the delayed rectifier of squid (Matteson and Swenson, 1986) and lymphocytes (Cahalan et al., 1985). More recently, studies using single channel recordings have shown that the mean channel open time is increased in the presence of Rb^+ in frog skeletal muscle delayed rectifiers (Spruce et al., 1989), rat skeletal muscle Ca-activated K channels (Demo and Yellen, 1990), and taenia coli Ca-activated K channels (Hu et al., 1989).

Matteson and Swenson (1986) reported that only permeant ions altered channel gating and that there was an apparent correlation between occupancy and gating, which led them to suggest that Rb^+ and other permeant ions affected gating by acting at a site in the pore (the occupancy hypothesis). On the other hand, because of the lack of voltage dependence of the slowing effect of external cations, it was proposed that Rb^+ (as well as Cs^+ and K^+) slows K channel closing by interacting with a site outside the membrane field (Clay, 1986, 1988). If this is true, the selectivity of the external site must be similar to the selectivity of the channel to explain the fact that only permeant ions affect gating. Furthermore, we have found that either external or internal Rb^+ slows closing, so there would have to be two sites outside the permeation pathway (one on the outer and one on the inner surface). Finally, we found that the

effect of either external or internal Rb^+ is voltage dependent, which is better explained by the simpler occupancy hypothesis as discussed in the next section.

Voltage Dependence of the Rb Effect

The rates of association and dissociation of a Rb^+ ion with a binding site in the pore are influenced by the membrane potential. In terms of the occupancy hypothesis, changes in the membrane potential could affect channel closing kinetics by modulating the monovalent cation occupancy of the channel. The voltage-dependent effect of *external* Rb^+ on channel closing would be consistent with this hypothesis if hyperpolarization decreases the Rb^+ occupancy of the channel. This interpretation requires that as the voltage goes negative the rate of Rb^+ dissociation from the site to the cell interior increases more than the rate of association of Rb^+ from the external solution to the site. Later we present a barrier model of the channel that is consistent with this explanation.

The situation is simpler to interpret if Rb^+ is only present internally, because in this case hyperpolarization *must* decrease occupancy because the association rate is reduced and the dissociation rate is increased. We have clearly shown that the closing kinetics of the K channel are slower when Rb^+ substitutes for K^+ as the main internal permeant cation (Figs. 7 and 8), and that the effect is voltage dependent. The observed effects of internal Rb^+ are significant for two reasons. First, the results show that Rb^+ can alter channel gating from either side of the membrane. A single, external site of action of Rb^+ is not supported by the fact that internal Rb^+ slows K channel closing. Second, the biexponential voltage dependence of the closing kinetics suggests a dual effect of voltage on the gating process. We believe that this result reflects an effect of voltage on both the Rb^+ occupancy of the channel and the rate of gate closing in the absence of monovalent ion occupancy of the channel.

Demo and Yellen (1990) have examined the voltage dependence of the effect of Cs^+ and Rb^+ on the gating of Ca^{2+}-activated K channels. Cs^+, which is known to block the channel in a voltage-dependent manner, produced a voltage-dependent effect on channel open time. In the presence of external Cs^+, hyperpolarization increased block, and it also increased the channel open time. From these experiments, it was concluded that Cs^+ affects gating by acting at a site in the pore. In addition, they found that external Rb^+ blocks the inward K current (indicating that it binds tightly in the pore) and that it also increases the probability that the channel is open.

Finally, we should consider how the voltage dependence of the Rb effect can be viewed in terms of the hypothesis that Rb^+ interacts with two sites outside the permeation pathway (one internal and one external site). With this model, we could speculate that voltage modulates the effect of Rb^+ on gating by altering the affinity of the Rb^+ binding site. Based on our results, negative voltages should decrease the affinity of both the internal and the external sites, and Rb^+ binding to the inner site should be eliminated by making the voltage sufficiently negative. This model is clearly more complex than the occupancy hypothesis, and therefore we prefer the simpler explanation. In the following section we show that certain calculations based on a barrier model of the K channel can be consistent with the occupancy hypothesis.

Voltage Dependence of the Probability of Site Occupancy

In the past, energy barrier models have been used to explain why channels do not behave like free diffusion pores (Woodbury, 1971; Hille and Schwarz, 1978; Begenisich and Cahalan, 1980). This kind of model has also been used to calculate the probability that a binding site in the pore is occupied by a monovalent cation, and to correlate occupancy with K channel closing kinetics (Matteson and Swenson, 1986). To determine if our data on the voltage dependence of the Rb^+ effect are consistent with the occupancy hypothesis, we have used a three-barrier, two-site model of the K channel to estimate the probability of site occupancy (P_o) at various voltages.

As described in the Methods, we used the barrier model to fit instantaneous *I-V* curves obtained with either external Rb^+ or K^+, or internal Rb^+ to estimate the parameters of the model. We have found that many different parameter sets can accurately fit the data. Two different examples are shown in Fig. 10, where we restricted the profile to symmetrical barriers (i.e., the six electrical distances were 1/6) and allowed the energy levels to vary. These two examples are shown because they produce different predictions concerning the voltage dependence of outer site occupancy, one consistent with the occupancy hypothesis and the other inconsistent. For the model on the left (Fig. 10, *A* and *B*) the following three features of the voltage dependence of P_o are consistent with the idea that Rb^+ ions affect gating when they are bound to this outer site. (*a*) As the membrane potential goes negative from −50 mV, P_o decreases in the presence of either internal or external Rb^+. (*b*) P_o is higher with external Rb^+. (*c*) With internal Rb^+, P_o approaches zero at negative membrane potentials. These calculations are consistent with the occupancy hypothesis, since our experimental results have shown that (*a*) the effect of Rb^+ on closing decreases as the membrane potential goes negative, in the presence of either internal or external Rb^+, (*b*) the channel closing rate is slower in the presence of external Rb^+, and (*c*) the slowing effect of internal Rb^+ can be completely removed at negative potentials. On the other hand, the model on the right (Fig. 10, *C* and *D*) is clearly inconsistent with the occupancy hypothesis because P_o increases as the membrane potential goes negative in the presence of external Rb. With our present results we cannot distinguish between these models, but the modeling shows that it is possible that the site where Rb^+ acts is in the pore.

The electrical distances need not all be equal to fit the instantaneous *I-V* curves, as shown in Fig. 11. In this case, the five independent electrical distances were varied in addition to the energy levels. Two examples are again shown, one consistent (Fig. 11, *A* and *B*) and one inconsistent (Fig. 11, *C* and *D*) with the occupancy hypothesis.

The effect of variations in the repulsion factor were also examined. In the models shown in Fig. 11, it is clear that the voltage dependence of P_o is influenced by the magnitude of the repulsion factor. Without any repulsion between ions, P_o in external Rb^+ is relatively independent of voltage from −140 to −50 mV. Increasing the repulsion factor increases the voltage dependence of P_o for external Rb^+ with a smaller effect on P_o for internal Rb^+. Repulsion factors > 10 produce little additional change in P_o. For the model shown in Fig. 11, *A* and *B*, a repulsion factor of 2 gives the best agreement with the occupancy hypothesis. This is equivalent to the repulsion of two ions in a medium of dielectric constant 20 at a distance of ~4 nm (Hille and

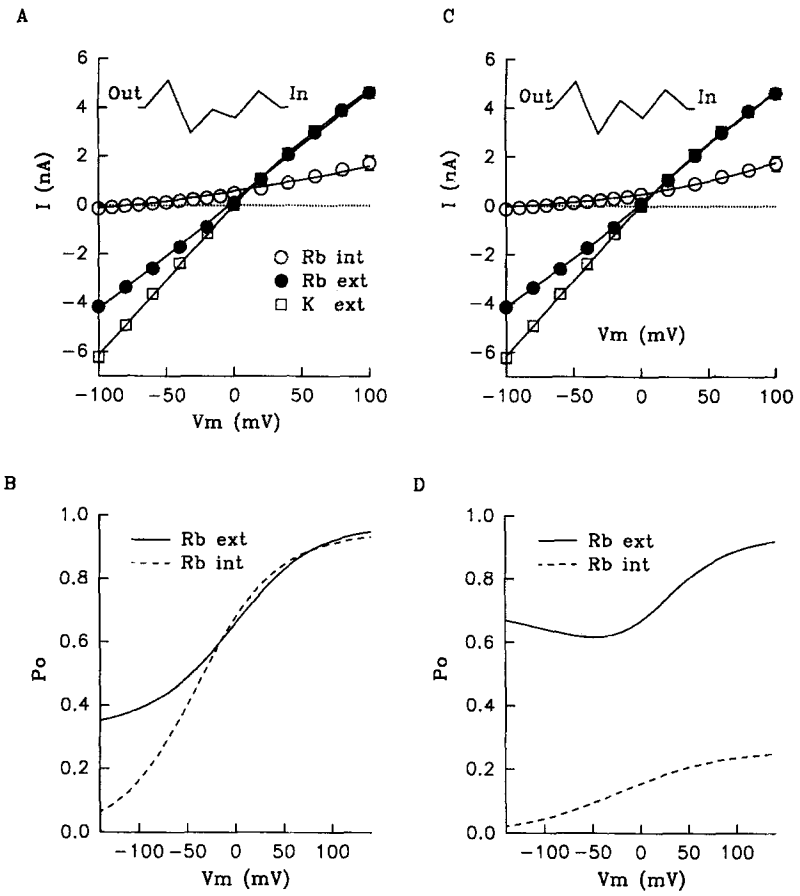

FIGURE 10. Symmetrical three-barrier, two-site model calculations of instantaneous *I-Vs* and the probability of site occupancy. (*A*) Instantaneous *I-Vs* obtained with external Rb^+ (*filled circles*), external K^+ (*open squares*), or internal Rb^+ (*open circles*). These data have been replotted from Figs. 3 and 9. The smooth lines through the data are the *I-V* relationships calculated with a three-barrier, two-site model. The inset illustrates the barrier profile for K. The energy profile had the following energy levels (in RT units, relative to the bulk solution), from outside to inside, for K^+: 7.786, −7.200, −0.576, −3.016, and 4.739; for Rb^+: 7.719, −7.945, 5.903, −3.791, and 5.812. The electrical distances for both K^+ and Rb^+ were all 1/6. (*B*) P_o for the outer site vs. the membrane potential for two ionic conditions: external (*continuous line*) or internal (*dashed line*) Rb^+. (*C*) The data points are the same as in *A*, as were the electrical distances. The profile for K was 7.704, −7.191, 2.259, −2.695, and 5.327, and for Rb was 6.655, −7.141, 7.486, −6.858, and 5.212. (*D*) P_o for the outer site vs. voltage for the model shown in *C*.

Schwarz, 1978). For the models shown in Fig. 10, P_o was nearly unaffected by changing the repulsion factor from 1 to 10. Changes in the repulsion factor produce different effects in these models because they have different energy levels at the inner site. In Fig. 10 the well is shallow so that the occupancy of the inner site is low at all

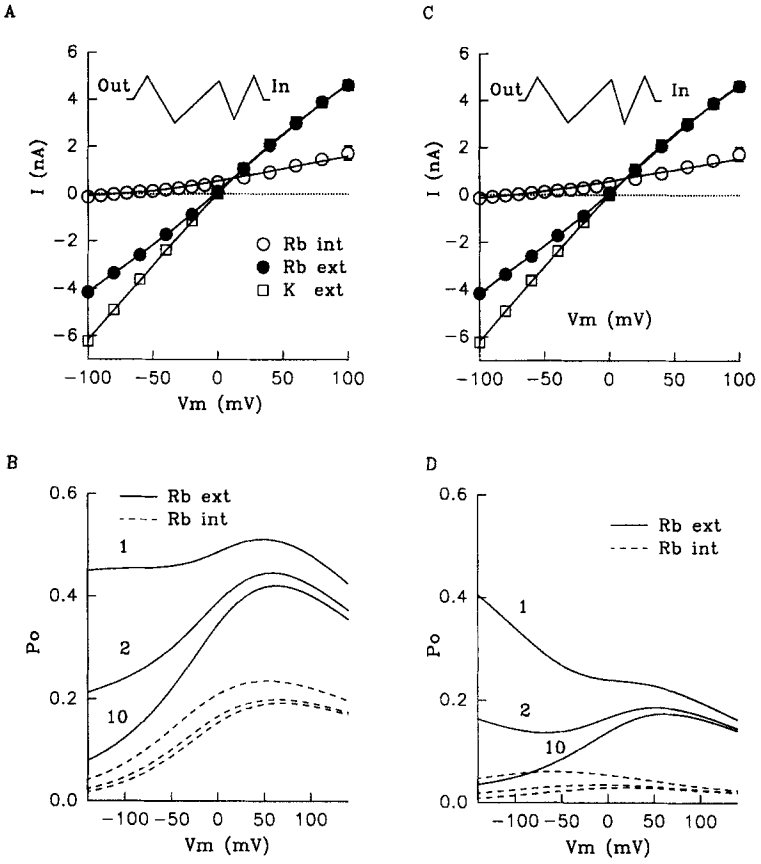

FIGURE 11. Barrier models with an asymmetrical energy profile. The data points for the instantaneous *I-Vs* are the same as in Fig. 10. (*A*) The electrical distances, from outside to inside, were 0.105, 0.213, 0.342, 0.114, 0.152, and 0.074. The energy levels, from outside to inside, for K were 7.098, −7.003, 5.563, −6.034, and 7.154, and for Rb were 7.091, −6.747, 6.356, −7.416, and 7.243. (*B*) P_o for the outer site vs. the membrane potential for both external (*continuous lines*) and internal (*dashed lines*) Rb. For each ionic condition, curves for three different repulsion factors are shown: 1, 2, and 10. (*C*) The electrical distances were 0.094, 0.237, 0.334, 0.098, 0.157, and 0.081. The energy levels for K were 6.954, −6.636, 6.412, −6.837, and 7.439, and for Rb were 6.859, −5.395, 7.093, −8.013, and 7.030. (*D*) P_o vs. voltage for the model shown in *C*.

voltages, and consequently the repulsion is not important. On the other hand, in Fig. 11 the inner well is deeper, the occupancy is higher, and the effect of repulsion is noticeable.

This work was supported by NIDDK grant DK-33212 to D. R. Matteson and by a fellowship to S. Sala from the Generalitat Valenciana.

Original version received 11 May 1990 and accepted version received 4 April 1991.

REFERENCES

Armstrong, C. M., and F. Bezanilla. 1974. Charge movement associated with the opening and closing of the activation gates of the Na channels. *Journal of General Physiology.* 63:533–552.

Ashcroft, F. M., M. Kakei, and R. P. Kelly. 1989. Rubidium and sodium permeability of the ATP-sensitive K^+ channel in single rat pancreatic β-cells. *Journal of Physiology.* 408:413–430.

Begenisich, T. B., and M. D. Cahalan. 1980. Sodium channel permeation in squid axons. I. Reversal potential experiments. *Journal of Physiology.* 307:217–242.

Blatz, A. L., and K. L. Magleby. 1984. Ion conductance and selectivity of single calcium-activated potassium channels in cultured rat muscle. *Journal of General Physiology.* 84:1–23.

Cahalan, M. D., K. G. Chandy, T. T. DeCoursey, and S. Gupta. 1985. A voltage-gated potassium channel in human T lymphocytes. *Journal of Physiology.* 358:197–237.

Chandler, W. K., and H. Meves. 1965. Voltage clamp experiments on internally perfused giant axons. *Journal of Physiology.* 180:788–820.

Clay, J. R. 1986. Potassium ion accumulation slows the closing rate of potassium channels in squid axons. *Biophysical Journal.* 50:197–200.

Clay, J. R. 1988. A new interpretation of the effects of monovalent cations on potassium channel gating in the squid axon. *Biophysical Journal.* 53:262*a*. (Abstr.)

DeCoursey, T. E., K. G. Chandy, S. Gupta, and M. D. Cahalan. 1987. Two types of potassium channels in murine T lymphocytes. *Journal of General Physiology.* 89:379–404.

Demo, S. D., and G. Yellen. 1990. Permeant ion effects on gating of the large conductance Ca-activated K channel from rat skeletal muscle. *Biophysical Journal.* 57:15*a*. (Abstr.)

Gay, L. A., and P. R. Stanfield. 1978. The selectivity of the delayed potassium conductance of frog skeletal muscle fibres. *Pflügers Archiv.* 378:177–179.

Hagiwara, S., and M. Yoshii. 1979. Effects of internal potassium and sodium on the anomalous rectification of the starfish egg as examined by internal perfusion. *Journal of Physiology.* 292:251–265.

Hille, B. 1973. Potassium channels in myelinated nerve. Selective permeability to small cations. *Journal of General Physiology.* 61:669–686.

Hille, B., and W. Schwarz. 1978. Potassium channels as multi-ion single-file pores. *Journal of General Physiology.* 72:409–442.

Hiriart, M., and D. R. Matteson. 1988. Na channels and two types of Ca channels in rat pancreatic β cells identified with the reverse hemolytic plaque assay. *Journal of General Physiology.* 91:617–639.

Hodgkin, A. L., and A. F. Huxley. 1952. The components of membrane conductance in the giant axon of *Loligo*. *Journal of Physiology.* 116:473–496.

Hu, S. L., Y. Yamamoto, and C. Y. Kao. 1989. Permeation, selectivity and blockade of the Ca^{2+}-activated potassium channel of the guinea pig taenia coli myocyte. *Journal of General Physiology.* 94:849–862.

Lewis, C. A., and C. F. Stevens. 1979. Mechanism of ion permeation through channels in a postsynaptic membrane. *In* Membrane Transport Processes. Vol. 3. C. F. Stevens and R. W. Tsien, editors. Raven Press, New York. 133–151.

Marchais, D., and A. Marty. 1979. Interaction of permeant ions with channels activated by acetylcholine in *Aplysia* neurons. *Journal of Physiology.* 297:9–45.

Matteson, D. R., and S. Sala. 1990. Rb slows K channel closing by acting at a site in the channel. *Biophysical Journal.* 57:509*a* (Abstr.)

Matteson, D. R., and R. P. Swenson, Jr. 1986. External monovalent cations that impede the closing of K channels. *Journal of General Physiology.* 87:795–816.

Nelson, M. T., R. J. French, and B. K. Krueger. 1984. Voltage dependent calcium channels from brain incorporated into planar lipid bilayers. *Nature.* 308:77–80.

Oxford, G. S., and D. J. Adams. 1981. Permeant cations alter K channel kinetics and permeability. *Biophysical Journal.* 33:70*a*. (Abstr.)

Oxford, G. S., and P. K. Wagoner. 1989. The inactivating K^+ current in GH_3 pituitary cells and its modification by chemical reagents. *Journal of Physiology.* 410:587–612.

Spruce, A. E., N. B. Standen, and P. R. Stanfield. 1989. Rubidium ions and the gating of delayed rectifier potassium channels of frog skeletal muscle. *Journal of Physiology.* 411:597–610.

Swenson, R. P., Jr., and C. M. Armstrong. 1981. K^+ channels close more slowly in the presence of external K^+ and Rb^+. *Nature.* 291:427–429.

Van Helden, D., O. E. Hamill, and P. W. Gage. 1977. Permeant ions alter endplate channel characteristics. *Nature.* 269:711–712.

Wagoner, P. K., and G. S. Oxford. 1987. Cation permeation through the voltage-dependent potassium channel in the squid axon. *Journal of General Physiology.* 90:261–290.

Woodbury, J. W. 1971. Eyring rate theory model of the current-voltage relationships of ion channels in excitable membranes. *In* Chemical Dynamics: Papers in Honor of Henry Eyring. J. O. Hirschfelder, editor. John Wiley & Sons, Inc., New York. 601–617.